

PAPER • OPEN ACCESS

## Noise emission from wind turbines in wake - Measurement and modeling

To cite this article: Franck Bertagnolio *et al* 2018 *J. Phys.: Conf. Ser.* **1037** 022001

View the [article online](#) for updates and enhancements.

### Related content

- [Performance and wake development behind two in-line and offset model wind turbines – "Blind test" experiments and calculations](#)  
Lars Sætran, Per-Åge Krogstad and Muyiwa Samuel Adaramola
- [Wake Conference 2015](#)  
Andrew Barney, Jens Nørkær Sørensen and Stefan Ivanell
- [Analysis of Power Enhancement for a Row of Wind Turbines Using the Actuator Line Technique](#)  
Robert Mikkelsen, Jens N Sørensen, Stig Øye et al.



**IOP | ebooks™**

Bringing you innovative digital publishing with leading voices to create your essential collection of books in STEM research.

Start exploring the collection - download the first chapter of every title for free.

# Noise emission from wind turbines in wake - Measurement and modeling

Franck Bertagnolio<sup>1</sup>, Helge Aa. Madsen<sup>2</sup> and Andreas Fischer<sup>3</sup>

<sup>1,2,3</sup> DTU Wind Energy, Frederiksborgvej 399, 4000 Roskilde, Denmark

E-mail: <sup>1</sup>frba@dtu.dk, <sup>2</sup>hama@dtu.dk, <sup>3</sup>asfi@dtu.dk

**Abstract.** The influence of the wake of an upstream turbine impinging another one located further downstream is studied focusing on the latter's noise emission. Measurement data are investigated in the form of surface pressure fluctuations acquired using microphones flush-mounted in a wind turbine blade near its tip, characterizing the noise sources. Numerical results from a wind turbine noise model are also included in the analysis. The wind speed deficit and increased turbulence levels of the wake flow are clearly observed. Surface pressure measurements strongly support the fact that turbulent inflow noise is increased. However, numerical results show that the wake velocity deficit reduces noise in certain circumstances. This can compensate, or even sometime more than compensate, the additional noise emission expected as a result of the wake turbulence. Furthermore, noise amplitude modulation appears to increase when the turbine is impacted by the wake flow.

## 1. Introduction

Wind turbine noise is an active area of research as it is considered as a key factor for social acceptance and further deployment of on-shore wind turbines (WT) in the future. Since WT are often deployed in small clusters or large wind farms, it is not unusual for a WT to operate in the wake flow originating from another (or several) WT located upstream.

The two main effects of an upstream WT wake on the downstream turbine aerodynamic characteristics are:

- The wind velocity deficit resulting from the energy extraction by the upstream turbine from the ambient wind flow forms a roughly cylindrical wake which is convected downstream. This flow deficit can be quite large and it may induce a great reduction of the energy production for the downwind turbine. The wake as it convects downstream is subjected to atmospheric turbulence, thus it does meander and it is distorted. It will eventually dissipate and disappear primarily under the action of turbulent diffusion, although this occurs over large distances (of the order of several kms). Therefore, the strength of its impact on the downstream turbine largely depends on the distance between the two turbines.
- On top of the pre-existing atmospheric turbulence, the wake flow contains additional turbulence structures generated by the blades of the upstream turbine in the form of shed and trailed vortices, tip vortices, as well as by the sharp velocity gradient between the wake core wind deficit and the largely undisturbed ambient flow outside the wake yielding to a locally unstable flowfield breaking down into turbulent vortices. Note that the meandering of the wake velocity deficit mentioned above will be felt as turbulent fluctuations (though with different spectral characteristics) when monitored at a fixed point in space.

Such wake has well-known important consequences on the impacted turbine's operation because of the added fatigue loads from the wake turbulence and sharp gradients of the inflow velocity field (e.g. in half-wake), as well as the energy losses because of the wind deficit [1]. However, the effects on the noise emissions resulting from wake operation have been scarcely studied [2, 3].

In this article, wake effects on noise emissions are investigated from two perspectives. Firstly, wind turbine measurement data provide quantitative information about physical quantities that are directly related to noise emissions. Secondly, a WT rotor noise model is used to corroborate these measurement data and study the influence of some parameters on the actual noise emissions according to this model.



## 2. The DANAERO experiment

As part of the DANAERO project conducted until year 2009 [4, 5], a 2.3MW NM80 WT with a 80m diameter rotor and a 60 m high tower was extensively equipped with multiple sensors in order to study its structural and aerodynamic characteristics. The turbine is located in Tjæreborg on the west coast of Denmark. One of its LM38.8 m blades was replaced by a test blade specifically manufactured for a series of measurement campaigns and equipped with a variety of additional sensors. The part of the instrumentation of the turbine and test blade relevant for the present study is briefly described below.

As all modern WT, this test turbine is equipped with a variety of sensors monitoring its operational conditions, e.g. rotational speed, blade pitch, power production, nacelle anemometer wind speed, through its SCADA system. At approximately 90% of the blade span, a Pitot tube is measuring the inflow onto the blade. Note that the angle of attack could not be extracted from this sensor due to a hardware system failure, but that the measured relative inflow velocity remained unaffected by this defect. Nevertheless, this angle of attack can be extrapolated from another Pitot tube mounted at 74% blade span. The calibration procedure is described in another article [6]. Furthermore, a nearby met mast located 313 m from the test turbine monitors the atmospheric conditions with several sonic and cup anemometers at various heights up to 93 m. All the above sensors are acquired at a sampling rate of 35 Hz. The measurement data are collected and continually stored into 10 mins files.

In addition, the test blade is equipped with flush-mounted surface pressure microphones distributed around a blade section located at 92% of its span. These are Sennheiser KE4-211-2 high-frequency microphones connected to an acquisition system sampling at 50 kHz. The microphone and housing set-up was calibrated using a similar configuration in laboratory conditions at Brüel & Kjær [6, 7]. The recorded microphone signals are also stored in separate files. As far as the present study is concerned, the primary quantity of interest related to noise emission is the surface pressure near the tip of the blade as measured by these microphones. Surface pressure is indeed a good measure of the emitted noise according to turbulent inflow and trailing edge noise theories [8, 9]. This is because surface pressure is directly connected to the noise sources which are the turbulent flow vortices, either the atmospheric turbulent vortices impacting the blade for turbulent inflow noise or the vortices developing inside the turbulent boundary layer along the blade for trailing edge noise. The main drawback of using surface pressure for evaluating the WT noise emissions is the fact that it only characterizes the noise sources, i.e. the turbulent vortices. Surface pressure does not include information about the actual dipole-type noise emission pattern from the blade hard surfaces, or the noise scattering at the leading and trailing edges. As a consequence, directivity effects are not included in such an analysis. Furthermore, atmospheric propagation effects are also ignored. Nevertheless, surface pressure remains a good indicator of noise emission, e.g. when comparing two different flow configurations as it is the case here when comparing the turbine operating in or out of the wake from an upstream turbine (see below).

In the present study, the analysis will concentrate on measurements conducted on September 1, 2009. Fig.1 displays the 10 mins average of various sensors' recordings during the time period of interest that day. This was a quite windy day with 10 mins averaged wind speeds ranging from approximately 9 to 15 m/s, see Fig. 1(e). The considered WT is part of a small farm and it is possible to sort out measurement data recorded when the turbine is operating in or out of the wake of the other turbines. As the day passed by, the wind direction gradually rotated by more than 60°. At some stage during this period of time, the test turbine became located directly in the wake of another WT located 253 m upstream, i.e. approximately 3 rotor diameters. Note that the test turbine lies exactly in the wake of the upstream turbine when the wind direction is 201°, that is approximately from 13:30 to 14:00 that day according to the mast sonic anemometer as displayed in Fig. 1(f). Remind that the effect of the wake on the test turbine may be perceived outside this time window as a result of the wake meandering.

It is worth mentioning here that the wake wind deficit can clearly be observed in Fig.1. Indeed, during the period of time 13:30-14:10 the wind speed measured by the nacelle anemometer in Fig. 1(a) as well as the turbine power output in Fig. 1(b), both being inherently correlated, exhibit temporarily significantly lower values. This may appear inconsistent with the wind speed simultaneously measured at the mast in Fig. 1(e) which remains largely unchanged during that period of time. These lower values can only be explained by a local wind flow deficit at the test turbine location that is most certainly caused by the wake of the upstream turbine.

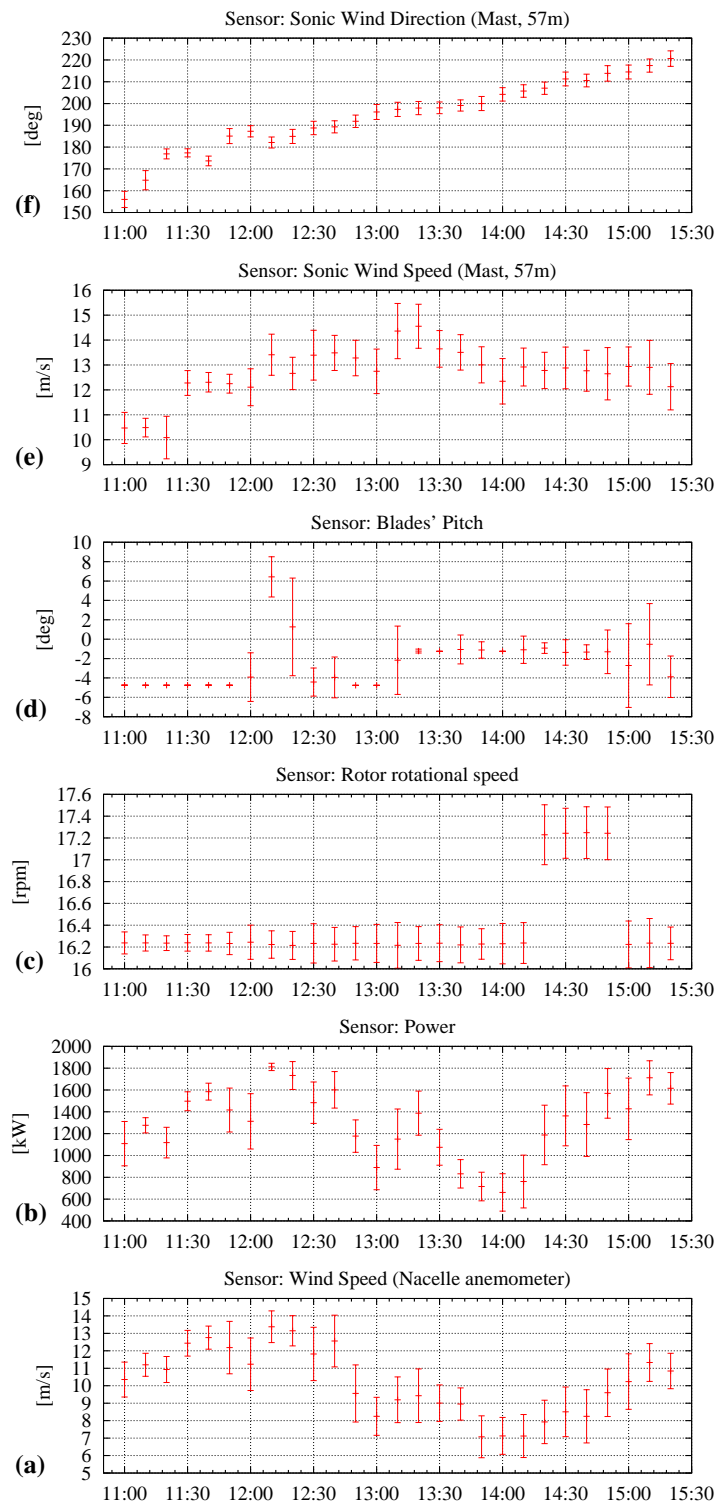


**Figure 1.** 10 mins average from various sensors with standard deviation recorded on September 1, 2009: (a) Nacelle anemometer wind speed, (b) Electrical power, (c) Rotational speed, (d) Blade pitch, (e) Mast sonic wind speed at 57 m height, (f) Mast sonic wind direction at 57 m height.

It should be noted that the WT is operated in a peculiar mode during the considered measurement campaign with the intent to obtain a constant rotor rotational speed. Indeed, the latter is fixed at 16.2rpm. Nevertheless, as observed in Fig. 1(c) and under the action of the turbine controller, it sporadically increases to 17.2rpm because the turbine torque exceeds the limit of the turbine converted/inverter system. In addition, two distinct constant blade pitch settings:  $-1.5^\circ$  and  $-4.5^\circ$  (positive nose down) are tested during the measurement period, see Fig. 1(d). Again, the controller sporadically increases the blade pitch when maximum power is exceeded.

To conclude this section, the post-processing of the measurement data is described below. To begin with, time-series of the turbine and mast data sampled at 35 Hz are synchronized with those of the high-frequency microphone data. Then, these time-series are split into sub-series of shorter time length as specified by the user. It is here chosen of the order of a few tenths of a second so that the atmospheric wind conditions impacting the test turbine as well as its operational conditions are not significantly changing during that period of time. Nonetheless, spectral analysis of the surface pressure sub-series measured with the high-frequency microphones can still reveal their low-frequency spectral contents. Because of spectral averaging (Welch's method [10]), the present analysis reaches out frequencies down to 100 Hz which are considered as low enough as far as WT noise emissions are concerned. Turbine and mast sensors are averaged over the time length of each sub-series. The sub-series are then filtered so that only configurations relevant for a specific study are selected. In the present context, it could be the test turbine being in or out of the wake of the upstream turbine using the wind direction sensor as displayed in Fig. 1(f), although using the sub-series' time length averaged values as defined above (the quantities displayed in the figure being 10 mins averaged). Any number of such constraints can be applied to the data set during this filtering process. The remaining sub-series are then binned according to some sensor averaged values, e.g. the turbine power output as it will be done later in this paper.

### 3. Wind turbine rotor noise model

Wind turbine rotor simulations presented in this work are performed using HAWC2 [11, 12] which is an aeroelastic code dedicated to the calculation of the aeroelastic behavior of WT for load predictions and design. It has been recently extended to model aerodynamic noise [13] from the blades. The reader is referred to the above references for further details about this model. Nonetheless, a few details relevant in the present context are reminded here.

The HAWC2 code does model various atmospheric effects including atmospheric turbulence. The latter is modeled by defining an instantaneous turbulent flow field inside a rectangular box large enough to encompass the rotor disk area using Mann model [14]. Frozen turbulence is assumed and this box is convected in time with the mean wind speed. In addition, wakes from upstream turbines can be simulated using the Dynamic Wake Meandering model [15]. This model takes into account the wake wind deficit from an upstream turbine and its meandering caused by the atmospheric turbulence. The additional wake turbulence is modeled by defining a secondary turbulence box which field is added on top of the previously mentioned atmospheric turbulent flow field.

Concerning the aerodynamic noise module of HAWC2, Amiet model [8, 16] is used to simulate turbulent inflow noise and a modified version of the TNO model for trailing edge noise [17, 18], including directivity and Doppler effects. Boundary layer properties needed for trailing edge noise modeling are computed and stored beforehand using a RANS-CFD code for 2D airfoil sections. Note that the turbulent inflow and trailing edge noise models are used independently (i.e. not as part of the above coupled HAWC2-Noise model) when analyzing the surface pressure measurements in Section 4. Nevertheless, the numerical inputs for these models are derived either from measurement data or from HAWC2 rotor aerodynamic calculations. In Section 5, the NM80 noise emissions are investigated numerically using the coupled HAWC2-Noise model. It should be reminded that HAWC2 is a temporal simulation code. At each time-step of a HAWC2-Noise simulation, noise spectra from the 3 blades, each with their individual inflow conditions, are calculated for a listener located on the ground directly downwind of the turbine at a distance equal to the tower height plus half the rotor diameter, as specified in the IEC 61400-11 standard for noise measurements [19]. Noise spectra are possibly A-weighted. These are then integrated over frequency and time-series of Sound Pressure Level (SPL) are calculated. It is important to note that non-weighted SPL is dominated by the low-frequency high-energy content of turbulent inflow noise, while A-weighted SPL is dominated by mid-frequencies originating from trailing edge noise.

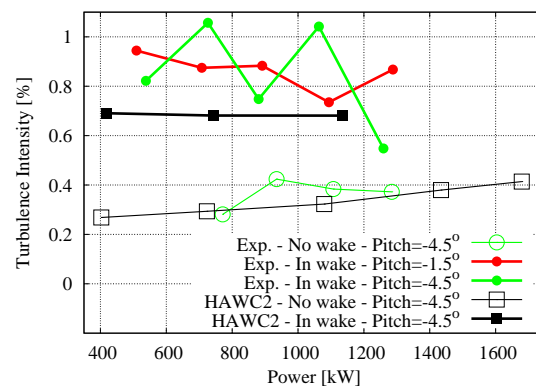


**Figure 2.** Turbulence intensity from relative inflow velocity at 90% blade span measured by the Pitot tube at that location on the NM80 blade or from HAWC2 computations as a function of power output.

#### 4. Comparisons of experimental and computational results

In this section, experimental data are investigated in order to analyze the effects of an impacting wake onto the WT operational characteristics as well as its noise emissions. This analysis is supported by numerical simulations using the HAWC2 code and its noise prediction module.

##### 4.1. Influence of an impacting wake on inflow turbulence

In order to evaluate the influence of the wake on the turbulence impacting the test turbine, the measurement data acquired by the Pitot tube at 90% blade span are analysed. Time-series of the measured relative inflow velocity are filtered and binned according to the procedure described in Section 2 and as detailed below.

The measurement data are filtered so that the mean rotational speed is 16.2 rpm. Two sets of data are distinguished using the wind direction from the mast sonic anemometer: one when the WT is directly lying in the wake of the upstream turbine, the other when it is not. Furthermore, the data are sorted according to the pitch angle of the blades which was alternatively fixed to two distinct values:  $-1.5^\circ$  and  $-4.5^\circ$  (positive nose down). Note that no data were acquired for the former value in the no-wake case. Finally, data are binned according to the electrical power output which should be a good measure of the instantaneous wind impacting the turbine averaged over the rotor disk area. Indeed, using the nacelle anemometer can sometimes be misleading because of the blades' wakes and various local flow features around the nacelle itself, in particular when considering short time-series as it is the case here (see below).

From the variance of the measured blade relative inflow velocity time-series, an inflow turbulence intensity (TI) at this specific blade radius can be computed by dividing the standard deviation of the above quantity by its mean value. Note that the variance is based on multiple 0.25 s long time-series, from the order of 10 to several hundreds of them depending on the results of the binning procedure. HAWC2-simulated time-series are truncated accordingly for the comparisons below. Because of the relatively short length of the considered time-series, this calculated TI is not necessarily representative of TI as understood in atmospheric physics where 10 mins time-series are typically used. Thus, the present values most probably underestimate the actual standard TI. Nevertheless, it is still representative of the physics that we are interested in, namely aerodynamic noise which is driven by flow disturbances with shorter time scales. This TI is displayed as a function of power in Fig. 2.

Firstly, it should be noted that the evaluated blade inflow TI is much lower than the actual standard atmospheric turbulence. The latter is estimated to be varying between 6% and 7% that day from an analysis of the wind speed time-series measured by the met mast's sonic anemometer at hub height, see Fig. 1(e). Besides the fact that the present TI is based on shorter time-series as explained above, the relative velocity is measured in a relative frame of reference moving with the blade and near its tip. Therefore, the mean value of the relative flow speed impinging the blade is quite larger than the atmospheric wind itself, while the amplitude of the turbulent fluctuations is



expected to be of the same order than that of the atmospheric turbulent wind. Secondly, a significant increase of the TI is observed when the turbine is operating in the wake of the upstream turbine.

Simulations performed with the HAWC2 code, with or without the action of the Dynamic Wake Meandering model (see Section 3), exhibit a similar tendency. Moreover, the computed values of the blade inflow TI for the turbine operating in or out of the wake match relatively well with the experimental data.

From the above, it can be concluded that the wake from an upstream turbine has a strong influence on the turbulent flow impacting a downstream turbine. In the present configuration, it is observed that the TI in the blade's frame of reference near the tip is roughly doubled. This should affect the blade surface pressures, and subsequently the noise emissions, as investigated below. Note that the study of the relative velocity alone might not give the full picture of the increased TI. The meandering of the wake velocity deficit will mainly impact the turbulence component in the flow direction, which is not significantly affecting the relative velocity.

#### *4.2. Study of wake wind deficit and wake turbulence effects on surface pressure spectra*

In this section, the effects of the test turbine operating in or out of the wake of the upstream turbine on the surface pressure measurement data are investigated. Then, these results are compared with noise model calculations in similar conditions as those of the experiment.

The measurement data are filtered and binned exactly in the same way as in the previous section when considering the blade relative inflow velocity measured by the Pitot tube. In Fig. 3, an increase of the surface pressure spectral energy at the leading edge is repeatedly observed when the turbine operates in wake conditions for all considered power bins. This is consistent with the additional wake turbulence impacting the turbine observed in the previous section. In contrast, it appears that the surface pressure measured near the trailing edge is nearly independent of the influence of the wake. However, as expected the trailing edge surface pressure is largely dependent on the blade pitch that is directly connected to the angle of attack at which the inflow impinges the considered airfoil section.

In order to model the measured surface pressure at the leading edge, Amiet's turbulent inflow noise model is used. As input, it requires the specification of the relative inflow velocity, the inflow TI and a turbulence integral length scale. The two first quantities are directly obtained from the Pitot tube's processed measurement data as described in Section 4.1. Concerning the second quantity, the following approach is used. Following the IEC 61400-1 standard [20], the atmospheric turbulence integral length scale  $L$  is defined as a linear function of the distance to the ground  $h$  as  $L = 0.7 \cdot h$  for  $h < 60$  m and constant above. An averaged value across the considered rotor disk area is evaluated as  $L = 35$  m. The previous approximation assumes a free flow without disturbances from an upwind WT's wake. As a rough estimation, the turbulent integral length scale in the wake flow is assumed to be half of the free flow value, i.e.  $L = 17.5$  m. Although this choice is quite arbitrary, it can be argued that a turbine's wake does add turbulent vortices to the pre-existing turbulent atmospheric flow. It can be expected that the initial characteristic size of these added vortices is lower than the characteristic scales of the energy-containing atmospheric turbulent vortices, before both kinds of vortices are broken down into smaller ones along the classical turbulence energy cascade. This is a rather heuristic approach to explain the actual mechanisms and above choices, but the only available so far. Surface pressure spectra measured near the leading edge are displayed in Fig. 3 (plots to the left of the figure).

Despite the above approximations, Amiet's model reproduces the increase of spectral energy when the turbine operates in wake. Nevertheless, the modeled spectral levels underestimate the measured ones. This is consistent with the fact discussed in the previous section that the calculated TI used to compute the present surface pressure spectra may underestimate the actual standard atmospheric value which should be used in Amiet's model. It may also be attributed either to the above turbulence length scale approximation or to Amiet's model itself which also includes numerous assumptions, e.g. that the airfoil profile section is a flat plate.

The modified TNO model [17] is used to reproduce the surface pressure near the trailing edge. Model input parameters, which consist of relative inflow velocity and angle of attack, are again extracted from the Pitot tube's processed measurement data. The results are displayed in Fig 3 (right plots). It can be seen that the modeled spectra appear shifted relatively to the measured surface pressure spectra. This behavior was already observed in a previous work by the authors [6]. The latter analysis indicates that this shift originates from the peculiar conditions on the actual blade

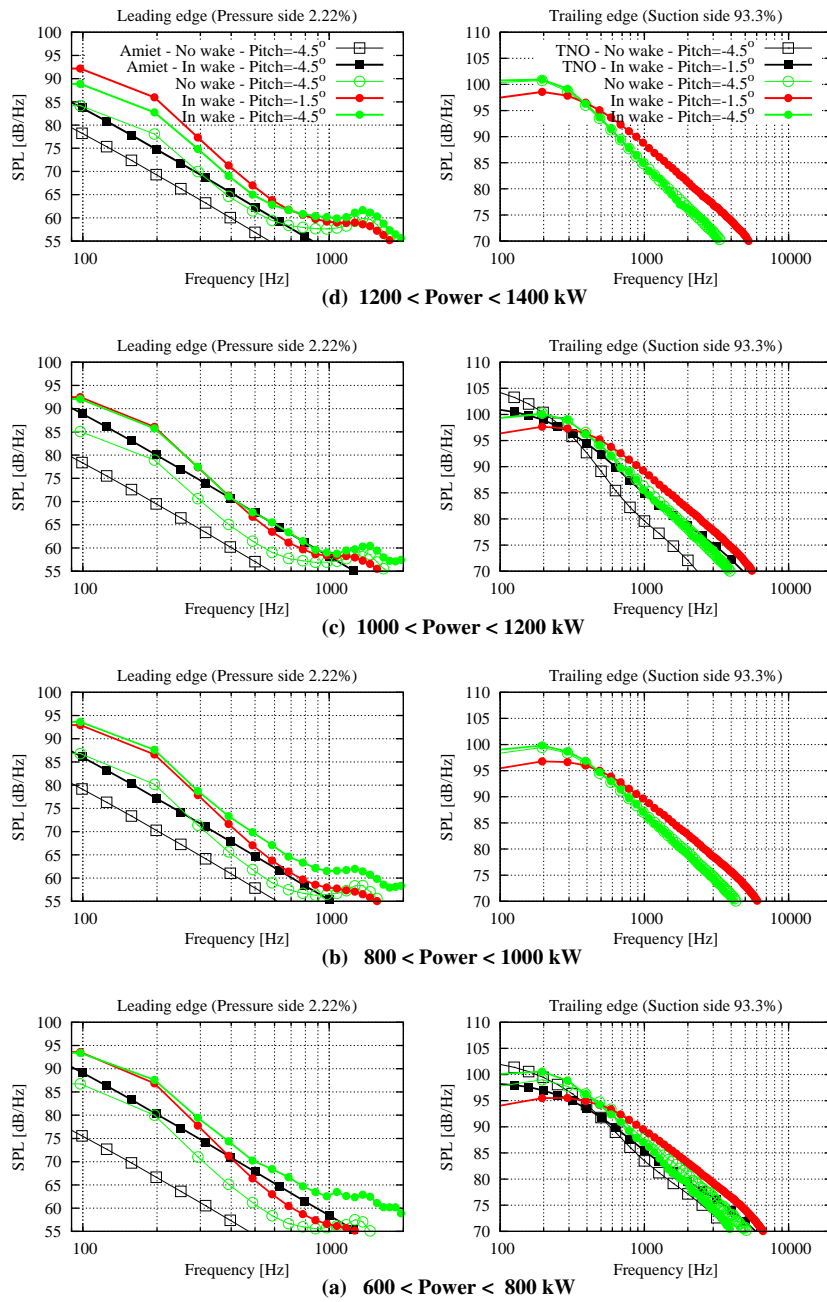


**Figure 3.** Surface pressure spectra measured by microphones near leading (left) and trailing (right) edges for a rotational speed of 16.2 rpm binned according to the turbine electrical power output  $P$ : (a)  $600 < P < 800 \text{ kW}$ , (b)  $800 < P < 1000 \text{ kW}$ , (c)  $1000 < P < 1200 \text{ kW}$ , (d)  $1200 < P < 1400 \text{ kW}$ . Black lines are Amiet's model (left) and modified TNO model (right).



which differ from the ideal conditions of the model. In particular, different transition mechanisms are suspected to have a significant influence on the spectral energy content of the boundary layer turbulence. There is also an uncertainty in the frequency response function of the pinhole microphones used for their calibration. Especially, the high frequency slope could be altered by the Helmholtz resonance. Nevertheless, the relative influence of the angle of attack on the spectra appears to be in agreement with the experiment.

### 5. Simulation of a controlled wind turbine in or out of wake and noise emissions

In this section, it is attempted to simulate a real-life WT subjected to the effects of the wake from an upstream turbine. Actual noise emissions in configurations that were not considered in the measurement campaign as investigated in the previous section are computed. The HAWC2-Noise model is used to simulate the NM80 turbine. It is important to note that a model of the turbine controller is also included in the present simulations. This controller may continuously modify the turbine rotational speed and/or blade pitch angle in order to optimize the power production as it does occur in reality, in contrast to the measurement campaign previously considered in this article for which these parameters are fixed.

All temporal simulations presented here are using identical turbulent flow fields, both for the main atmospheric turbulence and the wake turbulence. Two wake cases are considered: one for which the upstream turbine is located directly upwind of the turbine (referred to as 'full-wake' or FW for short), and one for which the upstream turbine is shifted relatively to the downstream turbine by half a rotor diameter (referred to as 'half-wake' or HW). In the former case, the downstream turbine is more likely, depending on the meandering process, to be fully exposed to the wake of the upstream turbine. In the latter case, the downstream turbine will be more often partially in or out of the wake than in the former case. Note that shifting the upstream turbine to the right or left yield similar conclusions, therefore only one set of results is presented here. Moreover, three different distances between the upstream and downstream turbines are considered: 3, 6 and 9 rotor diameters (denoted as '3D, 6D and 9D'). The wind speed (not including wake deficit) is set to 10 m/s for all calculations.

In the two next sections, time-series of both non-weighted and A-weighted SPLs are alternatively investigated. As explained in Section 3, the former are more representative of turbulent inflow noise, the latter of trailing edge noise.

#### 5.1. Non-weighted SPL and turbulent inflow noise

In Fig. 4, time-series of SPL emitted by the downstream turbine are plotted both for the FW and HW situations. The case without the influence of an upstream turbine wake is also plotted as reference. In HW, the emitted noise is decreasing as the distance between the upstream and downstream turbines increases. Yet, it is always larger than for the no-wake case because of the added wake turbulence. However, for the FW case and a distance between the turbines equal to 3D, the noise emission is actually lower than for larger distances, but also intermittently lower than the reference case without wake. This can be explained by the fact that the downstream turbine spends most of its time immersed in the wake. Indeed, this is a more likely situation than for the two other wake cases due to the proximity of the upstream turbine, and furthermore the downstream turbine is subjected to a stronger wake wind deficit. The controller of the downstream turbine reacts by reducing the rotor rotational speed as displayed in Fig. 6 and the blade tip speed is thereby also reduced. Since noise levels are strongly dependent on the blade tip speed, the above-mentioned peculiar behavior can be explained. The 6D and 9D FW cases behave like in the HW case. Note finally that the noise level variations are larger for the wake cases compared to the no-wake case because of the turbine going rapidly in and out of the wake because of meandering, which is even more true for the 3D case.

#### 5.2. A-weighted SPL and trailing edge noise

In Fig. 5, the time-series of A-weighted SPL are displayed for the same cases as above. In contrast to the non-weighted SPL, it can be seen that the FW 3D case exhibits even more important noise reductions compared to the no-wake case. The phenomenon yielding this effect is identical to the one explained above for the non-weighted SPL. All HW cases generate more similar noise levels since the downwind turbine is more prone to be out of the wake and is not dependent on the added wake turbulence as for the non-weighted SPL. Finally, it can be observed that the noise amplitude modulation due to the rotation of the blades is slightly stronger when the blade operates in wake. This is in line with a previous analysis of the inflow data set for the same turbine showing that the

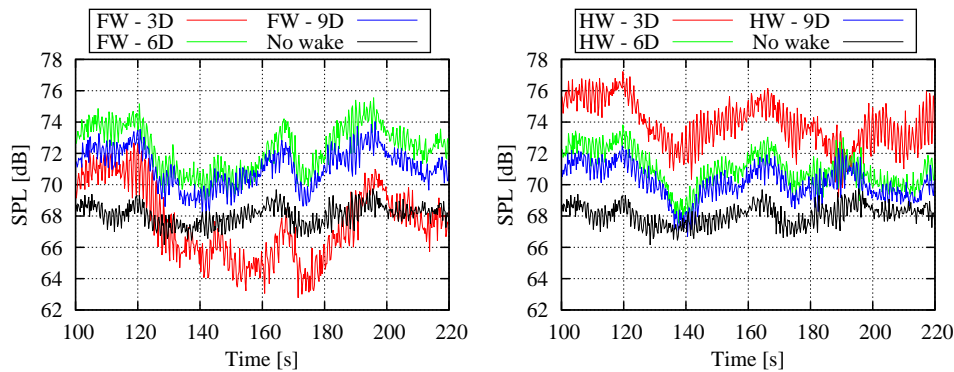


**Figure 4.** Time-series of Sound Pressure Levels from WT in the wake of another located at 3, 6 or 9 rotor diameters upstream (Left: Full wake, Right: Half wake) - Listener position is directly downstream of the rotor - SPL includes both turbulent inflow and trailing edge noise.

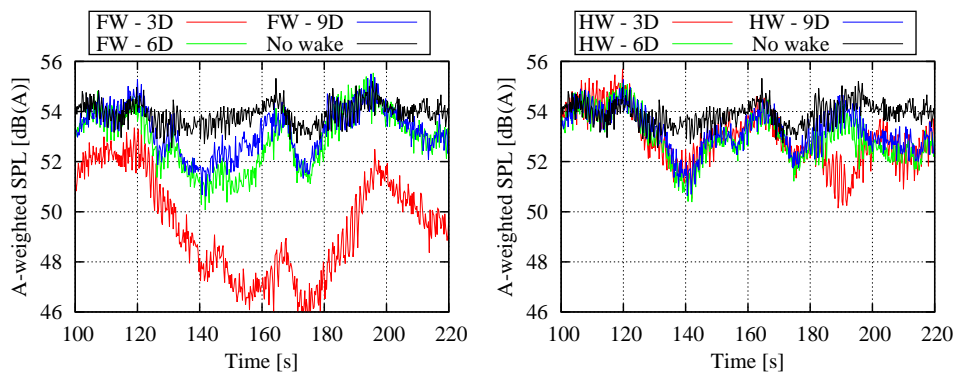


**Figure 5.** Time-series of A-weighted Sound Pressure Levels from WT in the wake of another located at 3, 6 or 9 rotor diameters upstream (Left: Full wake, Right: Half wake) - Listener position is directly downstream of the rotor - SPL(A) includes both turbulent inflow and trailing edge noise.

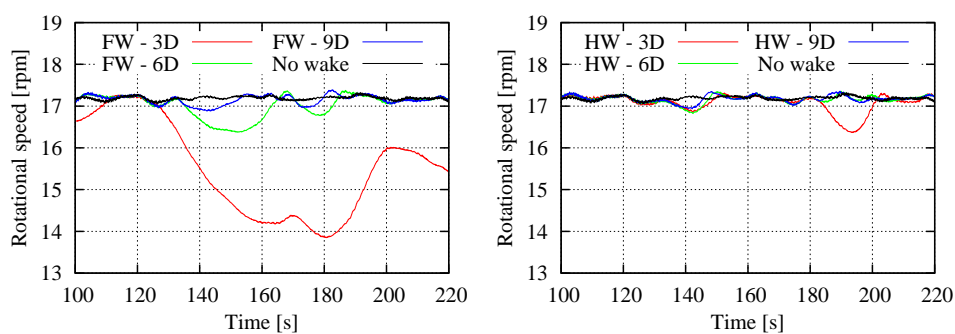


**Figure 6.** Rotational speed of WT in the wake of another located at 3, 6 or 9 rotor diameters upstream (Left: Full wake, Right: Half wake).

1P (i.e. periodic with a period corresponding to 1 rotor revolution) angle of attack variations causing amplitude modulations are substantially bigger for wake operation than for free inflow [3].

## 6. Conclusions

In this article, it is shown that the wake from an upstream turbine impacting a downstream one has a significant impact on the latter. Both its operational parameters and noise emissions are affected.

As expected, it is observed that a WT wake locally reduces the wind speed and the impacted turbine's power production due to the wake deficit. It is also observed that the turbulence intensity in the wake flow field is noticeably increased. These effects are verified using both field measurements and a WT computational model.

Furthermore, since noise emissions are not directly measured during the experimental campaign considered in this work, flush-mounted surface pressure microphones at a given airfoil section near the tip of the blade are used to characterize the noise sources. It is shown that the wake has a direct influence on the energy content of the surface pressure spectra at the leading edge and that it has an indirect influence on the surface pressure at the trailing edge through the velocity deficit induced by the wake and the subsequent reduction of the angle of attack on the blades.

While the above measurements were carried out at constant pitch and rotational speed, a computational study is conducted in order to evaluate the behavior of a real turbine subjected to a controller that drives both attributes in order to optimize its energy production. Noise emissions as experience downstream of the rotor are assessed. It is shown that wake operation yields an important increase of low-frequency noise for which turbulent inflow noise is the main contributor. However, this can be counter-balanced by the wind velocity wake deficit triggering a reduction of the rotational speed, especially if the distance between the two turbines is short. Indeed, noise emission typically scales with the rotational speed of the blades. Concerning high-frequency noise from trailing edge scattering, the impact of the wake is less significant in term of actual noise levels, but the wind deficit can still noticeably reduce the high-frequency energy content of the emitted noise when the two turbines are relatively close to each other. Note that these last conclusions may be affected by a different wind speed and/or turbulence intensity than the one considered in the present simulations.

## References

- [1] Castellani F, Buzzoni M, Astolfi D, D'Elia G, Dalpiaz G and Terzi L 2017 *Energies* **10**
- [2] Søndergaard L 2012 Noise from Wind Turbines under Non-standard Conditions *Inter-noise 2012* Conference Proceedings (New-York, USA)
- [3] Madsen H A, Bertagnolio F, Andreas A and Bak C 2014 Correlation of Amplitude Modulation to Inflow Characteristics *Inter-noise 2014* Conference Proceedings (Melbourne, Australia)
- [4] Madsen H A, Bak C, Paulsen U S, Gaunaa M, Fuglsang P, Romblad J, Olesen N A, Enevoldsen P, Laursen J and Jensen L 2010 The DAN-AERO MW Experiments - Final report Tech. Rep. Risø-R-1726(EN) Risø-DTU, Roskilde, Denmark
- [5] Madsen H A, Bak C, Paulsen U S, Gaunaa M, Fuglsang P, Romblad J, Olesen N A, Enevoldsen P, Laursen J and Jensen L 2010 The DAN-AERO MW Experiments 48<sup>th</sup> *AIAA Aerospace Sciences Meeting Including The New Horizons Forum and Aerospace Exposition (Proceedings)* AIAA Paper 2010-645 (Orlando (FL))
- [6] Bertagnolio F, Madsen H A, Bak C, Troldborg N and Fischer A 2015 *International Journal of Aeroacoustics* **14** 729–766
- [7] Guastavino R 2010 On-site Microphone Calibration for 'Low Noise Airfoil' EUDP Project J.nr. 64009-0272 Tech. Rep. (Private Communication) Brüel & Kjær Sound & Vibration Measurement A/S, Nærum, Denmark
- [8] Amiet R K 1975 *J. Sound Vib.* **41** 407–420
- [9] Howe M S 1978 *J. Sound Vib.* **61** 437–465
- [10] Welch P D 1967 *IEEE Transactions on Audio and Electroacoustics* **AU-15** 70–73
- [11] Larsen T J and Hansen A M 2006 Influence of Blade Pitch Loads by Large Blade Deflections and Pitch Actuator Dynamics Using the New Aeroelastic Code HAWC2 *Proc. of the European Wind Energy Conference and Exhibition* (Athens, Greece)
- [12] Larsen T J and Hansen A M 2007 How 2 HAWC2, The User's Manual Tech. Rep. RISØ-R-1597(ver.3-1) Risø-DTU, Roskilde, Denmark
- [13] Bertagnolio F, Madsen H A and Fischer A 2017 *Wind Energy* **20** 1331–1348
- [14] Mann J 1994 *Journal of Fluid Mechanics* **273** 141–168
- [15] Larsen G C, Madsen H A, Thomsen K and Larsen T J 2008 *Wind Energy* **11** 377–395 doi:10.1002/we.267
- [16] Paterson R W and Amiet R K 1976 Acoustic Radiation and Surface Pressure Characteristics of an Airfoil Due to Incident Turbulence 3<sup>rd</sup> *AIAA Aero-Acoustics Conference* Conf. Proceedings (Palo Alto, CA)
- [17] Bertagnolio F, Fischer A and Zhu W J 2014 *Journal of Sound and Vibration* **333** 991–1010
- [18] Fischer A, Bertagnolio F and Madsen H A 2017 *European Journal of Mechanics B - Fluids* **61** 255–262
- [19] 2012 International Standard, Wind Turbines - Part 11: Acoustic Noise Measurement Techniques IEC 61400-11 International Electrotechnical Commission, Geneva (CH)
- [20] 2005 International Standard, Wind Turbines - Part 1: Design Requirements IEC 61400-1 International Electrotechnical Commission, Geneva (CH)